

Particle Model of the Scattering-Induced Wigner Function Correction

M. Nedjalkov^{1,2}, P. Schwaha¹, O. Baumgartner¹, and S. Selberherr¹

¹ Institute for Microelectronics, TU Wien

Gußhausstraße 27-29/E360, A-1040 Vienna, Austria

² Institute for Parallel Processing, Bulgarian Academy of Sciences
Acad. G.Bontchev, Bl 25A, 1113 Sofia, Bulgaria

Abstract. The ability of accounting for quantum-coherent and phase-breaking processes is a major feature of the Wigner transport formalism. However, the coherent case is only obtained at significant numerical costs. Therefore, a scheme which uses coherent data obtained with a Green's function formalism has been developed. This scheme calculates the necessary corrections due to scattering using the Wigner approach and the associated Boltzmann collision models. The resulting evolution problem is not only theoretically derived, but simulation results are presented as well.

1 Introduction

Modeling and simulation of electronic devices is a part of science where knowledge of mathematics, physics, and electrical engineering is required simultaneously to design, analyze, and optimize these core components of the integral circuits. For the semiconductor industry it appears as the only alternative to the enormously expensive trial-and-error manufacturing approach. By means of device modeling and simulation the physical characteristics of semiconductor devices are explored in terms of charge transport and electrical behavior [2]. The progress in this field depends on the level of complexity of the transport models and the application of efficient numerical and programming techniques.

Physics provides a hierarchy of charge transport models summarized in Table 1. The ongoing miniaturization of devices forces the use of ever more sophisticated models to be able to capture all relevant effects and correctly calculate device behavior. The sophistication of the models, which increases from the bottom to the top is also characterized by an increase of the numerical complexity. The analytical models utilized during the infancy of microelectronics for circuit design were replaced by more rigorous drift-diffusion and hydrodynamic formulations, based on the moments of the Boltzmann equation. As these can be solved only numerically, corresponding deterministic methods have been developed.

When microelectronic devices enter the sub-micrometer scale, the moment equations fail, while the Boltzmann equation remains relevant. The Boltzmann equation provides a detailed classical picture of carrier evolution, where physical probability functions are associated with the various processes describing

Table 1. Carrier Transport Models

	MODEL	FEATURES
QUANTUM: nanometer and femtosecond scales	Green's Functions Method	Accounts for both spatial and temporal correlations
	Wigner equation; von-Neumann equation for the density matrix	Quantum-kinetic models of spatial correlations
	Quantum-hydrodynamic equations	Quantum corrections to classical hydrodynamics
CLASSICAL	Boltzmann transport equation	Comprehensive down to sub- μm and/or ps scales

carrier dynamics. The probabilistic nature along with the fact that the equation deals with a seven-dimensional phase space calls for a stochastic approach. The development of Monte Carlo (MC) methods for solving the equation can be considered as a major step in this field.

The nanometer and femtosecond scales of operation of modern devices give rise to a number of phenomena which are beyond purely classical description. These phenomena are classified in the International Technology Road-map for Semiconductors (ITRS, www.itrs.net) according to their importance to the performance of next generation devices. As is recognized in ITRS Table 122, 'Methods, models and algorithms that contribute to prediction of CMOS limits' are of utmost interest next to '... computationally efficient quantum based simulators'. Quantum models capable of describing not only purely coherent phenomena such as quantization and tunneling but also phase breaking processes such as interactions with phonons are especially relevant. The rising computational requirements resulting from the increasing complexity are a major concern for the development and deployment of these approaches. The harmony between theoretical and numerical aspects of the classical models is disturbed in the upper part of Table 1.

At the very top is the rigorous non-equilibrium Green's function approach (NEGF). It allows the simultaneous consideration of coherent processes of correlations in space and time and of phase breaking processes due to the lattice. However, because of numerical issues the applicability is restricted to stationary structures, basically in the ballistic limit [6]. The computational burden can be reduced by working in a mode space, obtained by separation of the problem into longitudinal and transverse directions. Furthermore, if the transverse potential profile along the transport direction remains uniform, the modes in these directions can be decoupled so that the transport becomes quasi-multidimensional. However, this is not the case for devices with a squeezed channel or with abruptly flared out source/drain contacts which require to consider two- and three-dimensional effects [3]. Phonon scattering has been included within a quasi-two-dimensional transport description [5]. Local approximations are commonly utilized in this case, where the phonon self-energy terms are diagonal in the coordinate representation. This is well justified for deformation

potential interaction, but must be adopted for interactions with polar phonons, surface roughness, and ionized impurities.

One level below in complexity are the Markovian in time (for pure states) approaches based on the density matrix or the unitary equivalent Wigner function. The recent interest in the semiconductor device society to simulation methods which rely on the Wigner transport picture is due to the ability of the latter to account for quantum-coherent and phase-breaking processes of de-coherence due to scattering of the carriers with phonons and other crystal lattice imperfections [4]. In this picture scattering can be accounted for in a straightforward way by using the Boltzmann collision models, while the coherent counterpart gives rise to a heavy numerical burden. This is in contrast to the Green's function approach which is numerically efficient in the cases of coherent transport.

2 Scattering-Induced Wigner Function Correction

We propose an approach [1] which combines the advantages of the two pictures. Green's function calculations of the coherent transport determined by the boundary conditions deliver the coherent Wigner function f_w^c .

$$\rho(x, x') = -2i \int G^<(x, x', E) \frac{dE}{2\pi}; \quad f_w^c(x, k_x) = \frac{1}{2\pi} \int ds e^{-ik_x s} \rho(x + \frac{s}{2}, x - \frac{s}{2}) \tag{1}$$

The lesser Green's function $G^<$ depends on the coordinates x, x' and energy E . The coherent Wigner function $f_w^c(x, k_x)$ is obtained from the density matrix $\rho(x_1, x_2)$ with the help of the center-of-mass transformation $x = \frac{x_1+x_2}{2}$, $s = x_1 - x_2$.

Furthermore, f_w^c is a solution of the coherent part of the Wigner-Boltzmann equation.

$$\begin{aligned} \frac{\hbar k_x}{m} \frac{\partial}{\partial x} f_w(x, \mathbf{k}) &= \int dk'_x V_w(x, k'_x - k_x) f_w(x, k'_x, \mathbf{k}_{yz}) \\ &+ \int d\mathbf{k}' f_w(x, \mathbf{k}') S(\mathbf{k}', \mathbf{k}) - f_w(x, \mathbf{k}) \lambda(\mathbf{k}) \end{aligned} \tag{2}$$

V_w is the Wigner potential. Phase-breaking processes are accounted for by the Boltzmann scattering operator with $S(\mathbf{k}, \mathbf{k}')$, the scattering rate for a transition from \mathbf{k} to \mathbf{k}' . $\lambda(\mathbf{k}) = \int d\mathbf{k}' S(\mathbf{k}, \mathbf{k}')$ is the total out-scattering rate. The coherent problem is obtained from (2) by setting the scattering rate S (and thus λ) to zero. In this case the \mathbf{k}_{yz} dependence remains arbitrary and can be specified via the boundary conditions. Formally the extrapolation must be such that $f_w^c(x, k'_x)$ is recovered by the integral over \mathbf{k}_{yz} . Moreover we want to cancel the Boltzmann scattering operator at the boundaries where standard equilibrium conditions are assumed. Hence, a Maxwell-Boltzmann distribution $f_{MB}(k'_{yz})$ is assumed in the yz directions, and the functions

$$f_w^c(x, \mathbf{k}') = f_w^c(x, k'_x) \frac{\hbar^2}{2\pi m k T} e^{-\frac{\hbar^2(k'^2_y + k'^2_z)}{2mkT}}; \quad f_w^\Delta(x, \mathbf{k}) = f_w(x, \mathbf{k}) - f_w^c(x, \mathbf{k})$$

can be introduced. The equation for the correction f_w^Δ is obtained by subtracting the coherent counterpart from (2). The correction is zero at the device boundaries, since the same boundary conditions are assumed for both cases.

3 Classical Limit

The obtained equation is approximated with the help of the classical limit.

$$\int dk'_x V_w(x, k'_x - k_x) f_w^\Delta(x, k'_x, \mathbf{k}_{yz}) = -\frac{eE(x)}{\hbar} \frac{\partial f_w^\Delta(x, k_x, \mathbf{k}_{yz})}{\partial k_x} \quad (3)$$

This approximation is valid for slowly varying potentials, so that the force $F(x) = eE(x)$ can only be a linear function within the spatial support of f_w^Δ . The force gives rise to Newton's trajectories

$$X(t) = x - \int_t^0 \frac{\hbar K_x(\tau)}{m} d\tau \quad K_x(t) = k_x - \int_t^0 \frac{F(X(\tau))}{\hbar} d\tau \quad (4)$$

initialized by $x, k_x, 0$. In this definition, if $t > 0$ the trajectory is called forward, otherwise it is a backward one. A backward trajectory crosses the boundary of the device at a certain time t_b , so that $f_w^\Delta(X(t_b), \mathbf{k}(t_b)) = 0$. The approximated equation can be transformed with the help of (4)

$$f_w^\Delta(x, \mathbf{k}) = \int_{t_b}^0 dt \int d\mathbf{k}' f_w^\Delta(X(t), \mathbf{k}') S(\mathbf{k}', \mathbf{k}(t)) e^{-\int_t^0 \lambda(\mathbf{k}(\tau)) d\tau} \quad (5)$$

$$+ \int_{t_b}^0 dt \left\{ \int d\mathbf{k}' f_w^c(X(t), \mathbf{k}') S(\mathbf{k}', \mathbf{k}(t)) - f_w^c(X(t), \mathbf{k}(t)) \lambda(\mathbf{k}(t)) \right\} e^{-\int_t^0 \lambda(\mathbf{k}(\tau)) d\tau}$$

into a Fredholm integral equation of the second kind with a free term given by the second row of (5) determined by f_w^c . The solution can be presented as a Neumann series with terms obtained by iterative application of the kernel to the free term. The series corresponds to a Boltzmann kind of evolution process, where the initial condition is given by the free term. The genuine mixed mode problem posed by the boundary conditions is transformed into a classical evolution of the quantum-coherent solution f_w^c . The latter, however, allows negative values and thus cannot be interpreted as an initial distribution of classical electrons: rather positive and negative particles initiate the evolution process. In this way the quantum information remains in (5) by the sign of the evolving particles. The boundary is still presented by t_b , however, it has a different physical meaning: it only absorbs particles, since trajectories with evolution time $t < t_b < 0$ do not contribute to the solution. In very small devices the carrier dwelling time can be so small that the probability for multiple scattering events tends to zero. In such cases the initial condition itself presents the correction f_w^Δ . In all other cases the evaluation of the initial condition is a necessary step for finding the solution. A particle approach derived for this purpose with the help of the numerical Monte Carlo theory is presented next.

4 Monte Carlo Approach

The general Monte Carlo task is to compute the averaged value $I(\Omega)$ of f_w^Δ in a given domain Ω of the phase space.

$$I = \int dx \int dk_x \theta_\Omega(x, k_x) f_w^\Delta(x, k_x) = \int dx \int dk_x \int dk_y \int dk_z \theta_\Omega(x, k_x) f_w^\Delta(x, \mathbf{k})$$

The domain indicator $\theta_\Omega(x, k_x)$ is unity, if its arguments belong to Ω , and 0 otherwise. We first consider the contribution of the second component $f_{0B}(x, k_x)$ of the initial condition which is the last term in (5).

$$I_{0B}(\Omega) = \int_{-\infty}^0 dt \int dx \int dk_x \int dk_y \int dk_z \frac{\hbar^2}{2\pi m k T} e^{-\hbar^2(k_y^2 + k_z^2)/2mkT} f_w^c(X(t), K_x(t)) \theta_\Omega(x, k_x) \lambda(K_x(t), \cdot) e^{-\int_t^0 \lambda(K_x(\tau), \cdot) d\tau} \theta_D(X(t))$$

The lower bound of the time integral has been extended to $-\infty$, since the introduced device domain indicator θ_D takes care for its correct value at t_b . The backward parametrization of the trajectories will be changed to forward ones aiming to achieve a more heuristic picture of the evolution of the real carriers. Two important properties of the trajectories will be utilized: (I) Any phase space point reached by the trajectory at any given time can be used for initialization, since it obeys a system of first order differential equations. A full notation of a trajectory $X(t), K_x(t)$ contains the initialization point: $X(t) = X(t; x, k_x, 0) = x^t, K_x(t) = K_x(t; x, k_x, 0) = k_x^t$. According to (I), the initialization can be changed from $x, k_x, 0$ to x^t, k_x^t, t so that $x = X(0, x^t, k_x^t, t), k_x = K_x(0, x^t, k_x^t, t)$. The second property (II) replaces for stationary transport the absolute clock by a relative one: trajectories are invariant with respect to a shift of both, initialization and parametrization time. Applying these properties consecutively gives:

$$X(\tau) = X(\tau; x, k_x, 0) = x^t = X(t - \tau; x^t, k_x^t, t) = X(-\tau; x^t, k_x^t, 0) = X^t(-\tau) \\ K_x(\tau) = K_x(\tau; x, k_x, 0) = k_x^t = K_x(t - \tau; x^t, k_x^t, t) = K_x(-\tau; x^t, k_x^t, 0) = K_x^t(-\tau)$$

With the introduced short notations X^t, K^t for the novel initialization $x^t, k_x^t, 0$ (of the same trajectory!) it holds that $x = X^t(-t), k_x = K_x^t(-t)$ (recall that $t < 0$). Finally, according to the Liouville theorem $dx dk_x = dx^t dk_x^t$. Here we need to discuss the involved domains in the phase space: the initially specified domain Ω is mapped backwards in time onto some domain $\Omega(t)$ so that the integration over x^t, k_x^t must be confined to $\Omega(t)$. However, we can augment the integration domain to the whole space, since by default trajectories defined by points outside $\Omega(t)$ will not enter Ω after time $-t$. For such trajectories $\theta_\Omega = 0$ so that the value I_{0B} remains unchanged by this step.

With these relations the expression for I_{0B} becomes

$$I_{0B} = \int_{t_b}^0 dt \int dx^t \int dk_x^t \int dk_y \int dk_z \frac{\hbar^2}{2\pi m k T} e^{-\hbar^2(k_y^2 + k_z^2)/2mkT} f_w^c(x^t, k_x^t) \theta_\Omega(X^t(-t), K_x^t(-t)) \lambda(k_x^t, k_y, k_z) e^{-\int_t^0 \lambda(K_x^t(-\tau), k_y, k_z) d\tau} \theta_D(x^t).$$

We change the sign of τ in the integral of the exponent, then replace t by $-t$, reorder the terms according their appearance in time and augment the expression by completing the probability densities in the curly brackets.

$$I_{0B} = \int_0^\infty dt \int dx^t \int dk_x^t \int dk_y \int dk_z \theta_D(x^t) \left\{ \frac{\hbar^2}{2\pi m k T} e^{-\frac{\hbar^2(k_y^2 + k_z^2)}{2m k T}} \right\} f_w^c(x^t, k_x^t) \quad (6)$$

$$\frac{\lambda(k_x^t, k_y, k_z)}{\lambda(K_x^t(t), k_y, k_z)} \left\{ \lambda(K_x^t(t), k_y, k_z) e^{-\int_0^t \lambda(K_x^t(\tau), k_y, k_z) d\tau} \right\} \theta_\Omega(X^t(t), K_x^t(t))$$

These conditional probabilities give rise to a MC algorithm for evaluation of $I_{0B}(\Omega)$. The computational task is now specified as the calculation of the value of $f_{0B}^{i,j} = f_{0B}(x^i, k_x^j)$ at a given point (x^i, k_x^j) . Then $\Omega = \Omega^{i,j}$ can be determined by the phase space area with a small volume $\Delta = \Delta k_x \Delta x$ around (x^i, k_x^j) so that $f_{0B}^{i,j} = I_{0B}(\Omega^{i,j})/\Delta$. Another peculiarity is the point wise evaluation of f_w^c giving rise to the approximation:

$$\int dx^t \int dk_x^t f_w^c(x^t, k_x^t) \simeq \sum_{i,j} f_w^c(i, j) \Delta$$

in (6). The following algorithm for evaluation of f_{0B} in the points of the mesh (i, j) is suggested:

1. Associate to each node i, j of the mesh in the phase space an initialized to zero estimator $\xi^{i,j}$.
2. The k_x^t, x^t integrals in (6) corresponds to a loop over i, j nodes; Initiate $l = 1, 2, \dots N$ trajectories from each node: the initial points can be fixed on the node or randomized within the cell; For each trajectory:
3. select the k_{yl}, k_{zl} values according to the term in the first curly brackets: algorithms for generation of Gaussian random numbers are well established. This step accounts for the k_y, k_z integrals.
4. The point x^t, k_x^t initializes the trajectory $K_x^t(t), X^t(t)$ at time $t = 0$. Along the trajectory $\lambda(K_x^t(t), k_{yl}, k_{zl})$ becomes a function of the time t . A value of the time $t = t_l$, the free flight time, is generated by the term in the last curly brackets by applying some of the well known algorithms utilized for device Monte Carlo simulation.
5. Add to the estimator $\xi^{i,j}$ at the mesh node i, j nearest to $K_x^t(t_l), X^t(t_l)$ the weight

$$w_l = f_w^c(x^t, k_x^t) \lambda(k_x^t, k_{yl}, k_{zl}) / \lambda(K_x^t(t_l), k_{yl}, k_{zl})$$

6. At the end of the i, j loop divide $\xi^{i,j}$ by N .

This algorithm can be further enhanced by a selection of the contribution term in the i, j sum according to $|f_w^c(i, j)|$. The current version, however, is flexible in providing information about the significance of particular device regions.

In a similar way the first term gives rise to the multiple integral

$$I_{0A} = \int_0^\infty dt \int dx^t \int dk_x^t \int dk_y \int dk_z \int dk' \theta_D(x^t) \left\{ \frac{\hbar^2}{2\pi m k T} e^{-\frac{\hbar^2(k_y'^2 + k_z'^2)}{2m k T}} \right\} f_w^c(x^t, k_x^t)$$

$$\left\{ \frac{S(\mathbf{k}', k_x^t, k_y, k_z)}{\lambda(\mathbf{k}')} \right\} \left\{ \lambda(K_x^t(t), \cdot) e^{-\int_0^t \lambda(K_x^t(\tau), \cdot) d\tau} \right\} \frac{\lambda(\mathbf{k}')}{\lambda(K_x^t(t), \cdot)} \theta_\Omega(X^t(t), K_x^t(t))$$

When compared to the previous case this algorithm accounts for an additional \mathbf{k}' integration related to the extra scattering event in I_{0A} :

1. Associate to each node i, j an estimator $\xi^{i,j}$.
2. Loop over i, j nodes corresponding to k_x^t and x^t integrals, and initiate $l = 1, 2, \dots N$ trajectories from each node:
3. select the k_{yl}', k_{zl}' values according to the term in the first curly brackets, thus accounting for the k_y, k_z integrals.
4. Select a wave vector according the term in the second curly-brackets. Input parameters are k_x^t, k_{yl}', k_{zl}' , the particular value of the after-scattering wave vector is denoted by $\mathbf{k} = k_{xl}^t, k_{yl}, k_{zl}$.
5. The point x^t, k_{xl}^t initializes the trajectory $K_{xl}^t(t), X_l^t(t)$ at time $t = 0$. Generate a free-flight time value t_l according to the term in the last curly brackets.
6. Add to the estimator $\xi^{i,j}$ at the mesh node i, j nearest to $K_{xl}^t(t_l), X_l^t(t_l)$ the weight

$$w_l = f_w^c(x^t, k_x^t) \lambda(k_x^t, k_{yl}', k_{zl}') / \lambda(K_{xl}^t(t_l), k_{yl}, k_{zl})$$

7. At the end of the i, j loop divide $\xi^{i,j}$ by N .

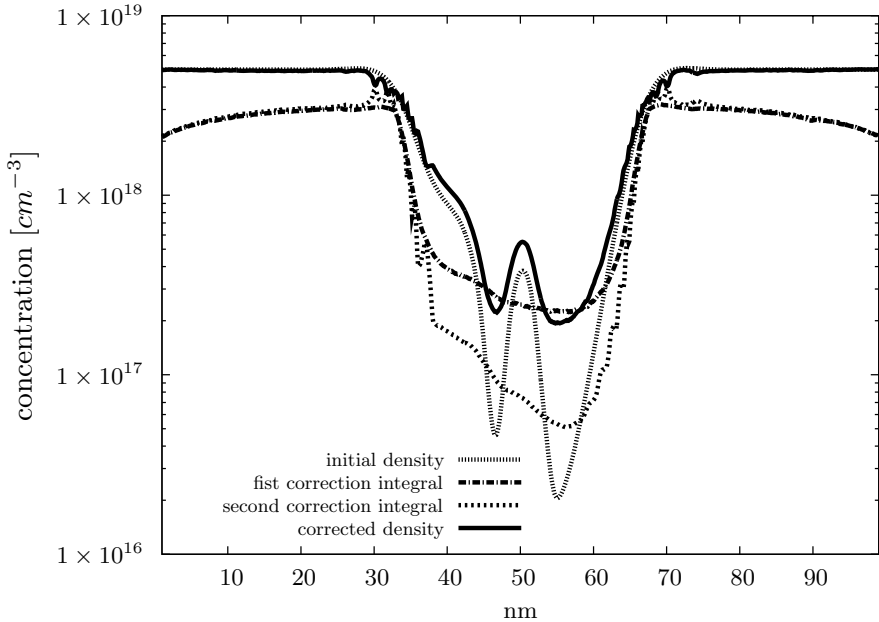


Fig. 1. Initial carrier density, densities due to first and second integrals, and corrected density calculated with $N = 10^4$. As expected theoretically the two integrals overlap deep in the equilibrium contacts. The scattering gives rise to an increase of the electron density in the well as compared to the coherent case.

5 Simulation Results

The developed algorithm has been applied to a GaAs resonant tunneling diode. The $4nm$ wide quantum well is surrounded by $1nm$ barriers with a height of $0.3eV$, applied is $0.3V$ bias. For such small device the initial condition represents the Wigner function correction. The results shown in Fig. 1 demonstrate that the physical effect of the scattering processes cannot be neglected as it would be done with a coherent approximation.

Acknowledgment

This work has been partially supported by the Österreichische Forschungsgemeinschaft (ÖFG), Project MOEL273 and by the Austrian Science Fund, special research program IR-ON (F2509).

References

1. Baumgartner, O., Schwaha, P., Karner, M., Nedjalkov, M., Selberherr, S.: Coupling of non-equilibrium Green's function and Wigner function approaches. In: Proc. Simulation of Semiconductor Processes and Devices, Hakone, Japan, pp. 931–934 (2008) ISBN: 978-1-4244-1753-7
2. Goodnick, S.M., Vasileska, D.: Computational electronics. In: Buschow, K.H.J., Cahn, R.W., Flemings, M.C., Kramer, E.J., Mahajan, S. (eds.) Encyclopedia of Materials: Science and Technology, vol. 2, pp. 1456–1471. Elsevier, New York (2001)
3. Luisier, M., Schenk, A., Fichtner, W.: Quantum transport in two- and three-dimensional nanoscale transistors: Coupled mode effects in the non-equilibrium Green's function formalism. *Journal of Applied Physics* 100, 043713–1–043713–12 (2006)
4. Querlioz, D., Saint-Martin, J., Do, V., Bournel, A., Dolfus, P.: Fully quantum self-consistent study of ultimate DG-MOSFETs including realistic scattering using Wigner Monte Carlo approach. In: Intl. Electron Devices Meeting, pp. 1–4 (2006)
5. Svizhenko, A., Antram, M.P.: Role of scattering in nanotransistors. *IEEE Trans. on Electron Devices* 50, 1459–1466 (2003)
6. Venugopal, R., Ren, Z., Datta, S., Lundstrom, M.S.: Simulating quantum transport in nanoscale transistors: real versus mode space approach. *Journal of Applied Physics* 92, 3730–3739 (2002)